

Convolutional Deblurring for Natural Imaging



Subhankar Chakraborty
EE17B031

Introduction



The problem of deblurring: definition and challenges

Introduction

- Blurring in many imaging modalities is caused by inadequate optical configuration in image acquisition
- One way to improve image perception is to deploy more sophisticated optical hardware. This is very expensive.
- On-the-fly correction of such images is important
- Both conditions of high accuracy and high speed are prerequisites

Point Spread Function

- In an imperfect optical system, a ray of light passing through the optical setup will spread over the image domain instead of converting to a single end point.
- This spreading effect is known as the point spread function (PSF)
- It suppresses sharp edges and leads to blurry observations.

Linear model for blurring

- The corresponding blur model is usually expressed by a linear convolution

$$f_B(x) = f_L(x) * h_{PSF}(x) + \eta(x), \quad (1)$$

- f_B is the blurry observation (sampled image)
- f_L is the latent sharp image (image to be recovered)
- h_{PSF} is the associated PSF kernel
- η is the noise contamination artifact

Deblurring/Deconvolution

- Refers to the restoration of the latent image from its blurry observation
- Inherently an ill-posed problem
- **Non-Blind Deconvolution:** When the PSF is given or known
- **Blind Deconvolution:** When the PSF is not known

Remaining Challenges

- High speed approaches are prone to ringing artifacts and/or losing fine image details
- Approaches with sophisticated deblurring are computationally expensive.
- CNN based models are limited by the blur modeling of natural images
- The majority of deconvolution methods involve complicated parameter tuning procedures which limit their generalization

1Shot-MaxPol



One-shot convolution filtering for blur image restoration

Contributions of the Paper

- The problems of image deblurring and denoising are decoupled for reconstruction
- A closed form of the deblurring kernel is designed as a linear combination of high-order FIR even-derivative filters.
- The generalized Gaussian distribution is used to model the PSF blur
- Proposes a new blind PSF estimation method using scale-space analysis in the Fourier domain.
- An adaptive tuning parameter is introduced based on the relative image entropy calculation to control the strength of deblurring

Work done

- Understanding the theory behind 1Shot-MaxPol
- Evaluation of the proposed method, 1Shot-MaxPol on many natural blurred images
- Implementation of maximum local variation (MLV) metric for no-reference sharpness quality assessment
- Complexity analysis of the proposed 1Shot-MaxPol

Proposed Decoupled Approach

- The paper proposes a new approach for symmetric PSF deblurring by correcting the fall-off of the high frequency band by means of frequency polynomial approximation
- The proposed method tries to regulate the effect of blurring operation in the frequency domain
- A dual filter representation in the spatial domain is defined to avoid directly manipulating the blur image in the frequency domain

Proposed Decoupled Approach

- The main approach here is to decouple denoising and blur correction by defining two separate convolutional filters in the dual spatial domain

$$h_D(x) = h_{PSF}^{-1}(x) * h_{Denoise}(x)$$

- $h_D(x)$ is the decoupled filter. Convolution of $h_D(x)$ with f_B yields the latent approximation $\bar{f}_L(x) = h_D(x) * f_B(x)$
- Denoising and deblurring are decoupled, enabling them to be individually addressed during recovery.

Inverse Deconvolution Kernel Design

- The inverse filter is defined as the inverse Fourier transform of the inverse PSF response $h_{PSF}^{-1}(x) = \mathcal{F}^{-1}\{1/\hat{h}_{PSF}(\omega)\}$.
- Directly calculating the inverse Fourier will introduce Gibbs artifacts.
- To avoid this, a dual representation in both Fourier and spatial domains is defined by approximating the inverse PSF response in the Fourier domain by a series of frequency polynomials.

$$\frac{1}{\hat{h}_{PSF}(\omega)} \approx \sum_{n=0}^N \alpha_n \omega^{2n}$$

Inverse Deconvolution Kernel Design

- $\{\alpha_n\}_{n=1}^N$ are determined by fitting the inverse PSF response to the polynomial series up to certain frequency range

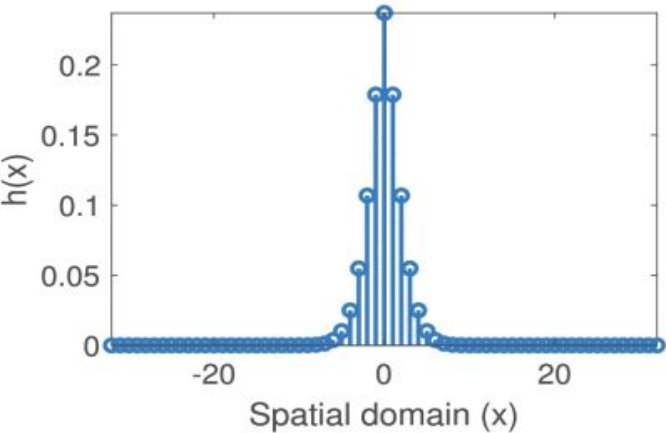
$$\arg \min_{\alpha_n} \left\| \frac{1}{\hat{h}_{PSF}(\omega)} - \sum_{n=0}^N \alpha_n \omega^{2n} \right\|_2, \quad \omega \in [0, \omega_T]$$

- The dual representation of the inverse filter defined in above can be equally represented by

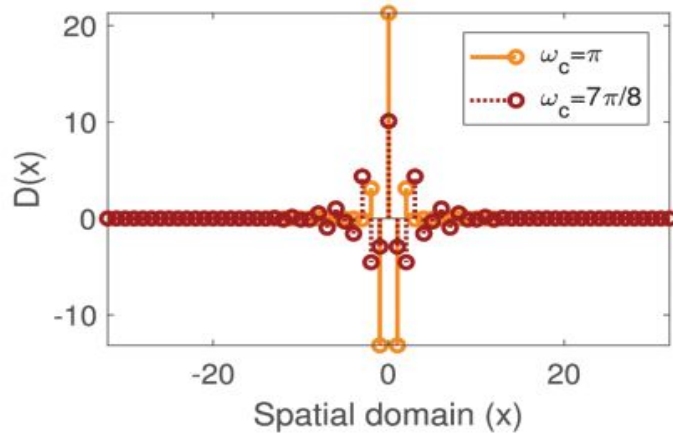
$$h_{PSF}^{-1}(x) \approx \delta(x) + \sum_{n=1}^N \alpha_n (-1)^n \frac{\partial^{2n}}{\partial x^{2n}}$$

Inverse Deconvolution Kernel Design

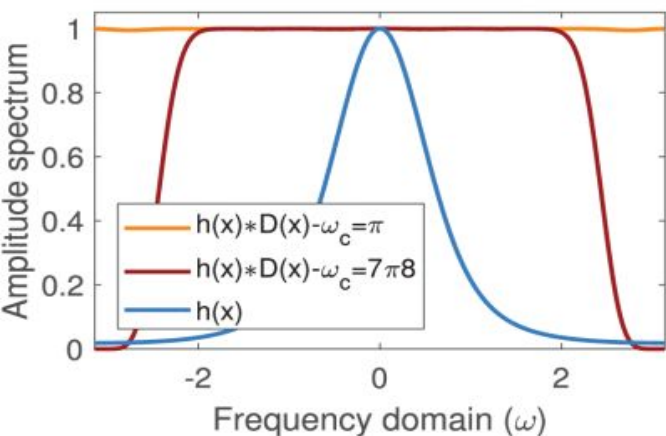
- The continuous derivative operators can be numerically approximated using Finite Impulse Response (FIR) convolution filters $h_{PSF}^{-1}[k] = \delta[k] + D[k]$.
- $D[k] = \sum_{n=1}^N \alpha_n (-1)^n d^{2n}[k]$ is the associated FIR deblurring kernel. Here, $d^{2n}[k]$ is the discrete approximation to the $2n^{\text{th}}$ order derivative operator applied in the bounded continuous domain $x \in [-T, T]$
- For numerical solution of the derivative filters, the MaxPol library is used



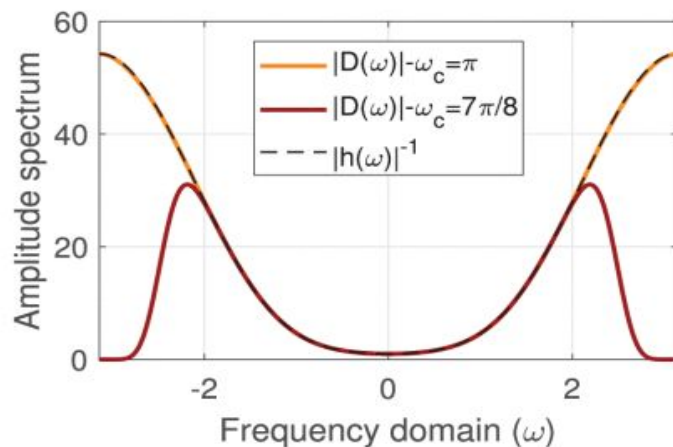
(a) GG-Blurr kernel h



(b) Inverse deblurring kernel D



(c) Spectrum of $|\mathcal{F}\{h * D\}|$

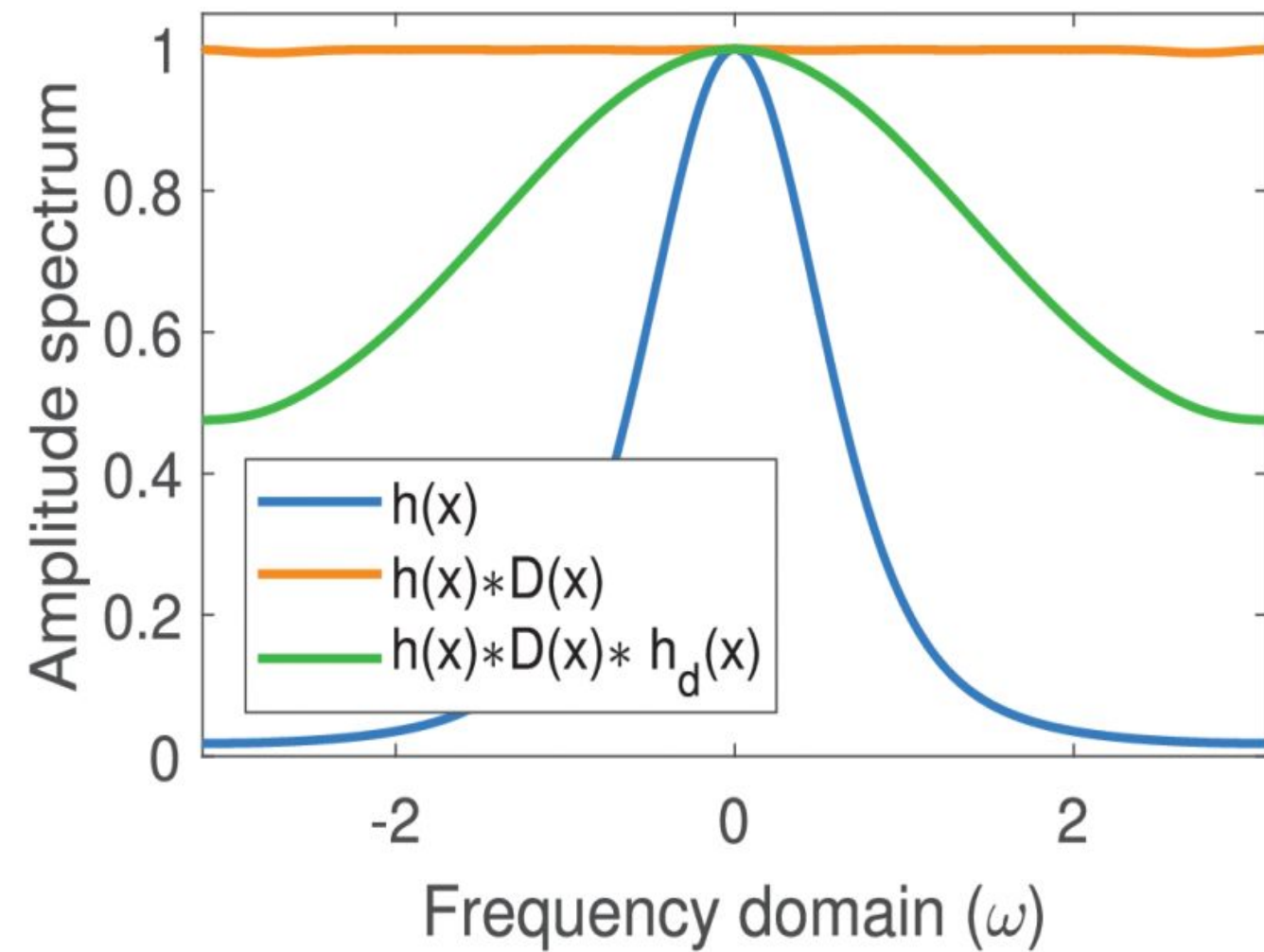


(d) Spectrum of inverse kernel

Inverse deconvolution $D(x)$ kernel design. The blurring kernel here is a generalized Gaussian form with parameters $\alpha=2$ and $\beta=1.5$. This type of kernel is usually common in many real imaging applications such as optical aberration and turbulent medium blur. Derivatives up to the 14th order are used, i.e., $N=7$, to design $D(x)$ with two different cut-offs $\omega_c=\{7\pi/8, \pi\}$

Decoupled Smoothing Filter

- The whole idea of decoupled design in is to balance the amplitude fall-off of high frequency components caused by the PSF kernel.
- If no denoising/cut-off is considered, all of the frequency domain will be deconvolved according to the inverse kernel response.
- Once the image is deconvolved by an inverse filter, similar symmetric blur kernels with less blur scale than that considered for deconvolution are applied (convolved) for denoising.
- This guarantees that the fall-off of the high frequency amplitude will be balanced between noise cancellation and amplifying meaningful edge information.



Adding a denoising filter h_d as a decoupled module after fall-off correction of the blurring kernel.

Two Dimensional Deblurring Framework

- For imaging applications, the previous section must be extended to 2D
- The PSF blur in many optical imaging systems is considered to be rotationally symmetric
- It is generally assumed that the blur operator is independently applied in both dimensions (separable mode). The linear model hence becomes

$$f_B(x, y) = f_L(x, y) * h_{PSF}(x) * h_{PSF}(y) + \eta(x, y)$$

$$f_R(x, y) = h_D(x) * h_D(y) * f_B(x, y)$$

- The energy level of the blurring kernel is usually unknown a priori for natural imaging problems.

Adaptive Level Tuning

- A tuning parameter $\gamma \in [0, 1]$ is defined to control the significance of the deconvolution level: $f_R(x, y) = f_B(x, y) + \gamma \nabla_D f_B(x, y)$
- $\nabla_D f_B(x, y) = f_B(x, y) * [D_x + D_y + D_{xy}]$ gives the reconstructed image edges
- $D_{xy} = D_x * D_y$ is the crossed deconvolution operator independently applied to the horizontal and vertical axes
- The significance level γ is calculated as the relative ratio of two image entropies

$$\gamma \triangleq \frac{E(f_B)}{E(\nabla_D f_B) + T}$$

Blur Modeling and Estimation



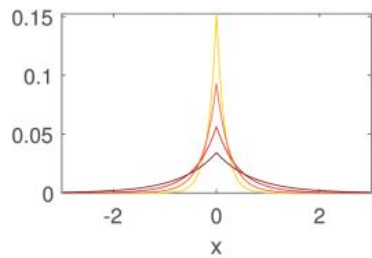
The generalized Gaussian distribution. Blind PSF Estimation.

Modeling Blur by Generalized Gaussian (GG)

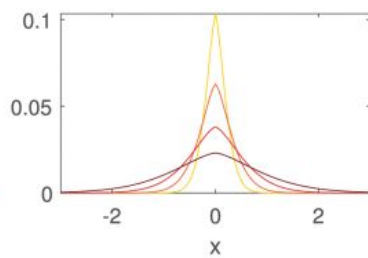
- The generalized Gaussian (GG) distribution is given by

$$h_{GG}(x) = \frac{1}{2\Gamma(1 + 1/\beta)A(\beta, \sigma)} \exp - \left| \frac{x}{A(\beta, \sigma)} \right|^\beta$$

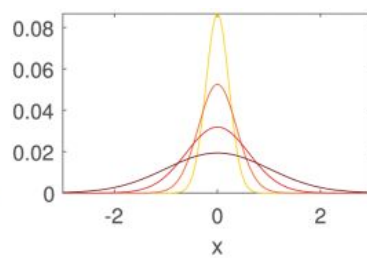
- The spectral responses of the blur kernels are inversely related to their scales, where low scales maintain wider frequencies for transformation.
- A common approach is to employ such kernels in a non-blind fashion for image deconvolution. The shape and the scale are the two different characteristics that fit different blur applications



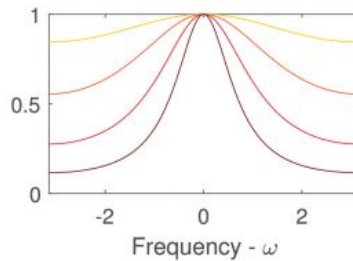
(a) $h_{GG}(x), \beta = 1$



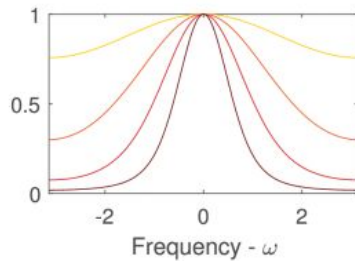
(b) $h_{GG}(x), \beta = 1.5$



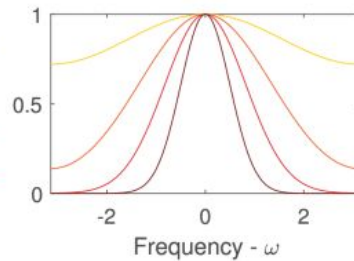
(c) $h_{GG}(x), \beta = 2$



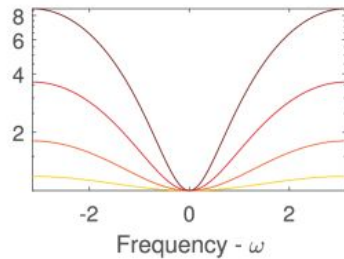
(d) $|\hat{h}_{GG}(\omega)|$



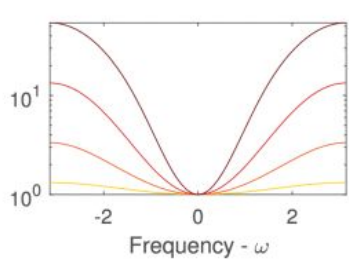
(e) $|\hat{h}_{GG}(\omega)|$



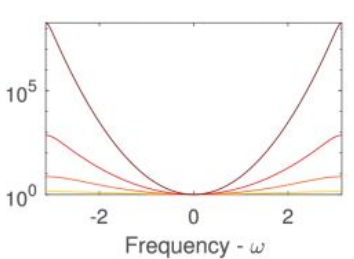
(f) $|\hat{h}_{GG}(\omega)|$



(g) $|\hat{h}_{GG}(\omega)|^{-1}$



(h) $|\hat{h}_{GG}(\omega)|^{-1}$



(i) $|\hat{h}_{GG}(\omega)|^{-1}$

Generalized Gaussian kernel considered for blurring model. The kernels are generated with different shapes β and scales α . The range of selected scales here is $\alpha = \exp(-0.75, -0.5, \dots, 0.75)$ and correspond to the transition of color shades from dark to yellow, respectively. The impulse responses are shown in the first row, amplitude spectrum in second row, and the inverse amplitude spectrum in the third row.

Blind PSF Estimation

- Relies on image scale-space analysis using two different scales. The originally sampled image $f_B(x, y)$ and its down-sampled version $f_B(sx, sy)$ for $s > 1$.
- This scale is reversed in the Fourier domain, i.e., $\hat{f}_B(\omega_x/s, \omega_y/s)$
- The coordinates are transferred from Cartesian to polar $(\omega_x, \omega_y) \mapsto (r, \theta)$ to obtain $\hat{f}_B(r/s, \theta)$
- The blur image is integrated along a closed circle to calculate its radial spectrum and the terms are expanded using the linear convolution model which gives

$$\int_0^{2\pi} \hat{f}_B(r/s, \theta) d\theta = \int_0^{2\pi} \hat{f}_L(r/s, \theta) \hat{h}(r/s, \theta) + \hat{\eta} d\theta$$

- Natural images (without blur) usually follow a decay spectrum of $\hat{f}_L \approx 1/r$

Blind PSF Estimation

- The noise is assumed to be additive white Gaussian noise (AWGN)
- Substituting these assumptions, we get $\int_0^{2\pi} \hat{f}_B(r/s, \theta) d\theta \approx \int_0^{2\pi} \frac{s}{r} \hat{h}(r/s, \theta) d\theta + c$
where $c \propto SNR^{-1}$. For good quality images, $(c \rightarrow 0)$
- A ratio spectrum of two different scales of original and subsampled domains is defined
$$R(r) \equiv \frac{\int_0^{2\pi} \hat{f}_B(r, \theta) d\theta}{\int_0^{2\pi} \hat{f}_B(r/s, \theta) d\theta} \approx \frac{\int_0^{2\pi} \hat{h}(r, \theta) d\theta + cr}{s \int_0^{2\pi} \hat{h}(r/s, \theta) d\theta + cr}$$
- The right-hand-side (RHS) is used to fit a certain blur model as a prior knowledge of the equation, where the data fidelity term is provided by approximating the ratio $R(r)$ using two radial spectra of different image scales.

Evaluation and Experiments



Metric used for evaluation, Qualitative results

Maximum Local Variation

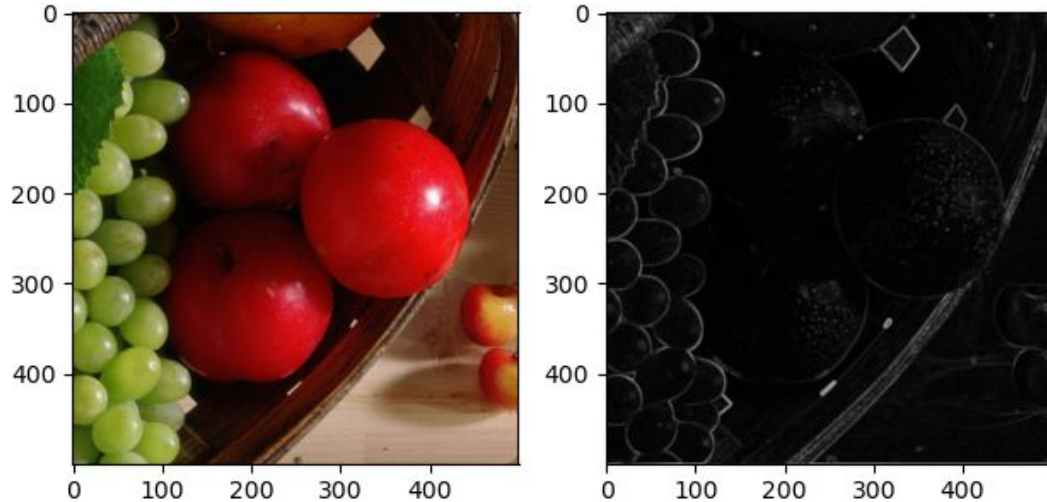
- A fast metric for No Reference-Focus Quality Assessment (NR-FQA)
- Higher values indicate better focus resolution
- For a grayscale image I with pixel value at coordinates (i, j) represented by $I_{i,j}$, the MLV value at (i,j) is defined as

$$\psi(I_{i,j}) = \{\max |I_{i,j} - I_{x,y}| \mid x = i-1, i, i+1, y = j-1, j, j+1\}$$

- MLV changes in the range of 0–255
- The MLV values for grayscale images are normalized to be in the range $[0,1]$
- Standard deviation of the distribution is used to measure sharpness

MLV Map Generation

- A colour image of shape $M \times N$ is converted into a grayscale image



$$\Psi(I) = \begin{pmatrix} \psi(I_{1,1}) & \cdots & \psi(I_{1,N}) \\ \vdots & \ddots & \vdots \\ \psi(I_{M,1}) & \cdots & \psi(I_{M,N}) \end{pmatrix}$$

Weighted MLV Map

- By changing the distribution in such a way that the tail part becomes heavy, the distribution can be used to evaluate the sharpness more effectively.
- This can be done by assigning higher weights to the larger MLV pixels by generating the weighted MLV map

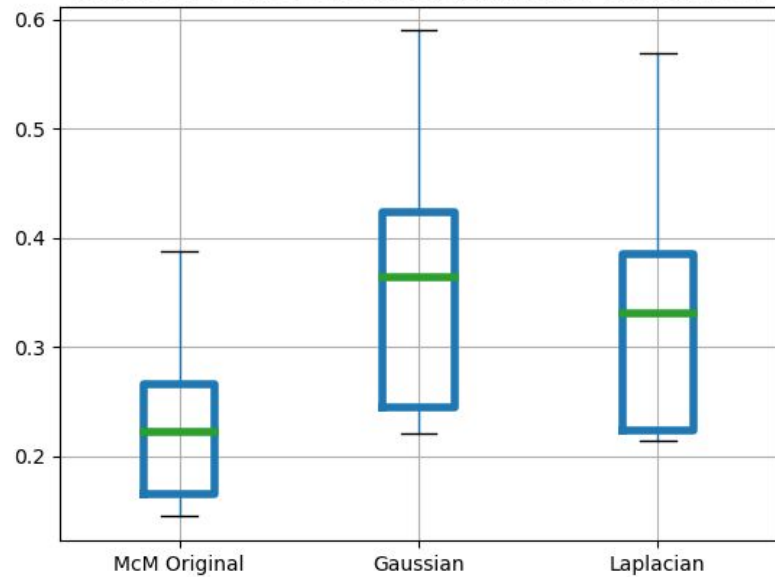
$$\Psi_w(I) = \begin{pmatrix} w_{1,1}\psi(I_{1,1}) & \cdots & w_{1,N}\psi(I_{1,N}) \\ \vdots & \ddots & \vdots \\ w_{M,1}\psi(I_{M,1}) & \cdots & w_{M,N}\psi(I_{M,N}) \end{pmatrix}$$

- $w_{i,j} = e^{\eta_{i,j}}$ and $\eta_{i,j}$ is the rank of $\psi(I_{i,j})$ when sorted in ascending order from 0 to 1
- Standard deviation of weighted MLV distribution is used to measure sharpness

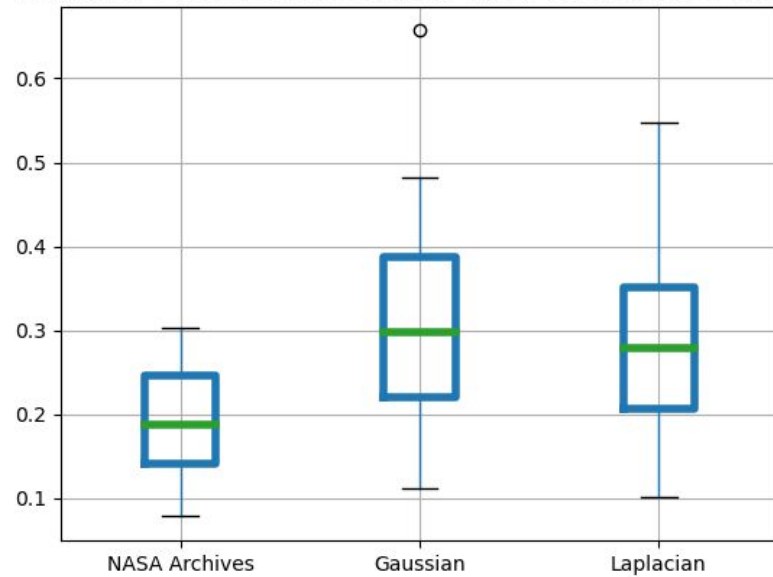
Results

- All images generated with scale factor $s=4$
- Results generated for both the Gaussian and Laplacian blur models
- Standard deviation of the weighted MLV distribution used as the sharpness score
- Box plots of each dataset before the deblurring and after the deblurring with both the Laplacian and Gaussian blur models is presented
- Some qualitative results also provided

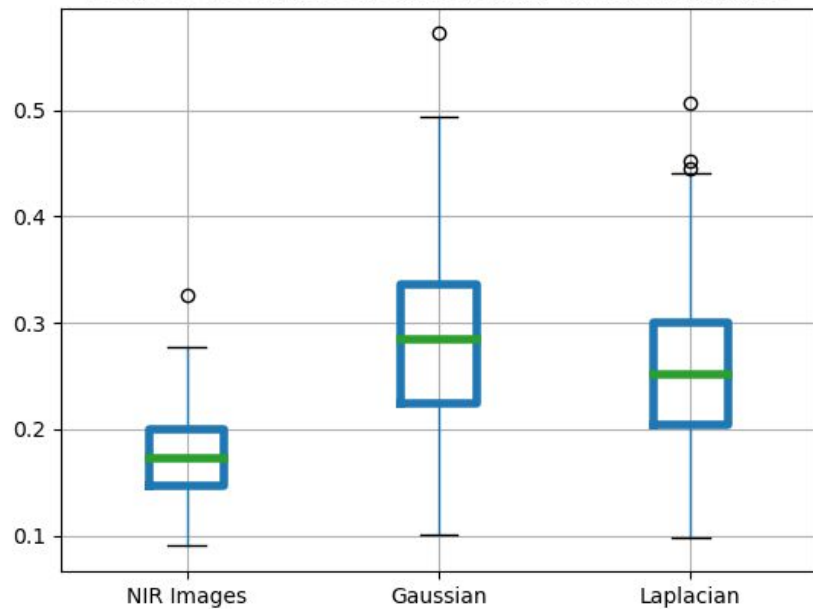
Boxplot of σ values calculated using Ψ_w for McM dataset



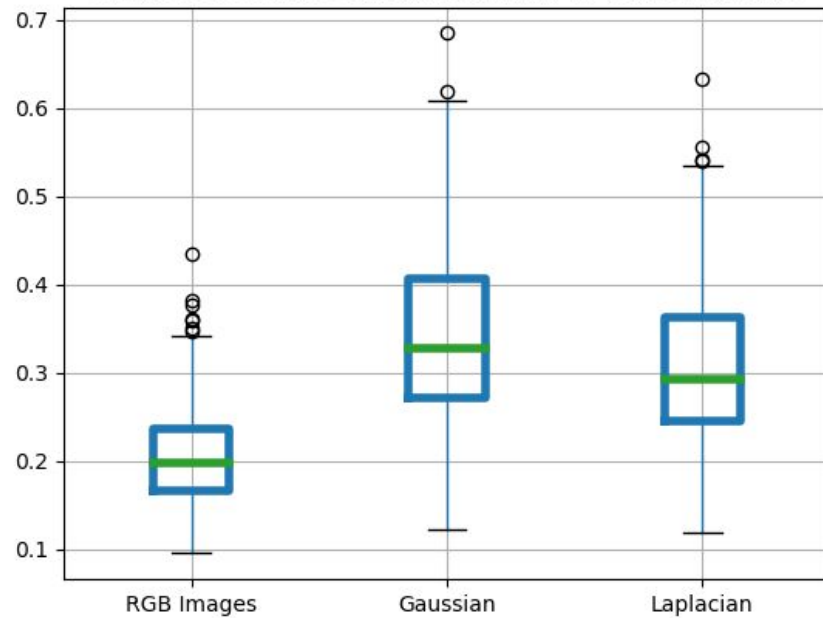
Boxplot of σ values calculated using Ψ_w for NASA Archives images



Boxplot of σ values calculated using Ψ_w for NIR images



Boxplot of σ values calculated using Ψ_w for RGB images



Original



Gaussian



Laplacian



Original cropped



Gaussian cropped



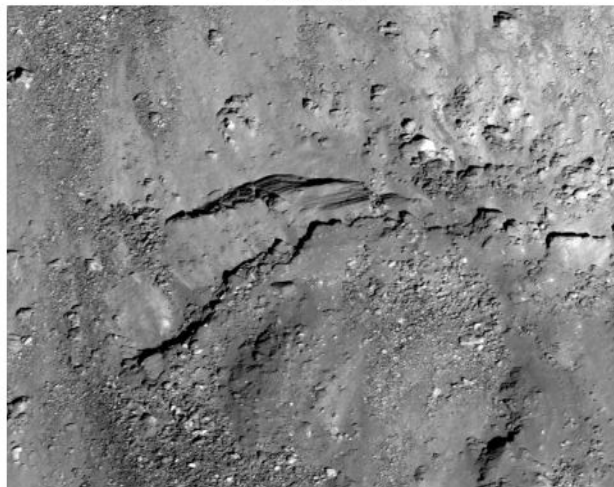
Laplacian cropped



Original



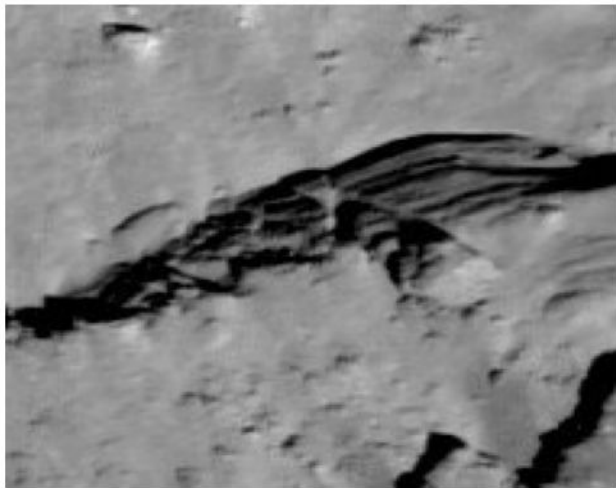
Gaussian



Laplacian



Original cropped



Gaussian cropped



Laplacian cropped



Original



Gaussian



Laplacian



Original cropped



Gaussian cropped



Laplacian cropped



Original



Gaussian



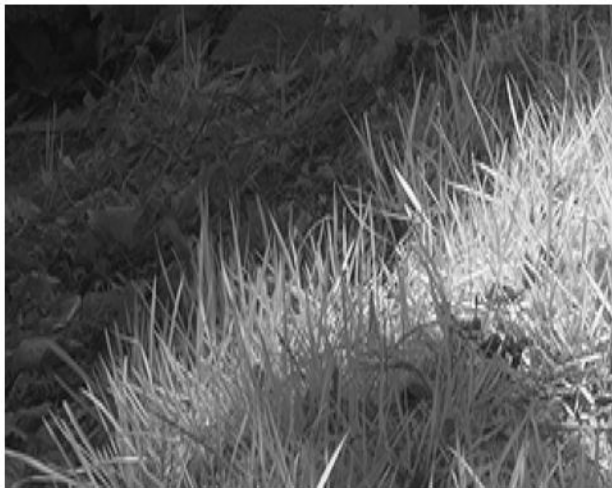
Laplacian



Original cropped

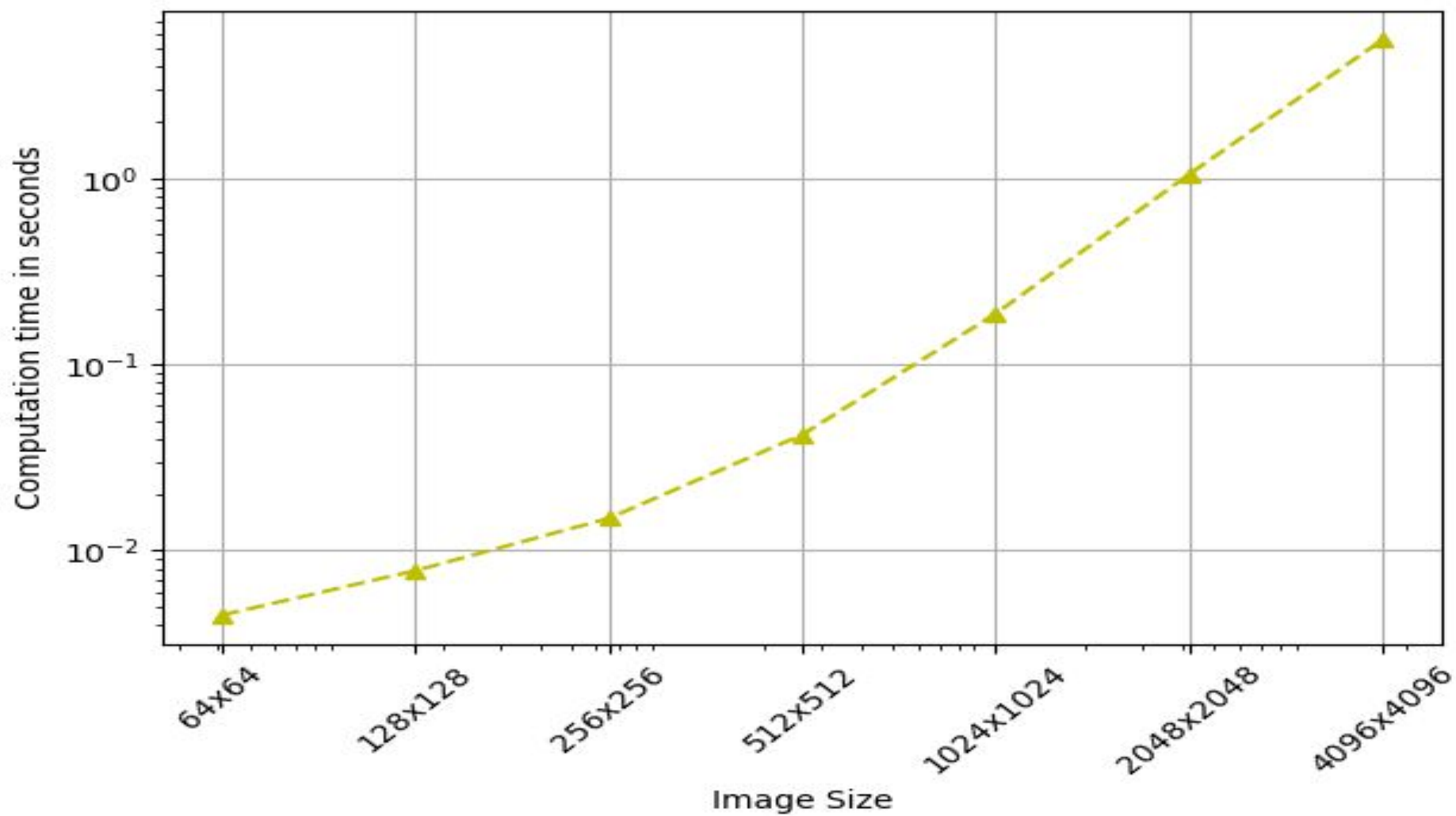


Gaussian cropped



Laplacian cropped





Conclusions

- The paper proposes a novel algorithm to correct symmetric optical blur
- The denoising part is decoupled from the deblurring part enabling users to use a denoising model of their choice depending on the use case
- The dual filter representation in the spatial domain helps prevent ringing effects in the final image by not manipulating the image in the frequency domain
- The PSF statistics are calculated using the novel approach of scale-space analysis of image blur in the Fourier domain

References

- Hosseini, Mahdi S., and Konstantinos N. Plataniotis. "[Convolutional deblurring for natural imaging](#)." IEEE Transactions on Image Processing 29 (2019): 250-264.
- Bahrami, Khosro, and Alex C. Kot. "[A fast approach for no-reference image sharpness assessment based on maximum local variation](#)." IEEE Signal Processing Letters 21.6 (2014): 751-755.

The End

